Photoion Spectroscopy in the 4*d* Giant Resonances of the Lanthanides

Ch. Dzionk, W. Fiedler, M. v. Lucke, and P. Zimmermann

Institut für Strahlungs- und Kernphysik, Technishe Universität Berlin, Hardenbergstrasse 36, D-1000 Berlin 12, West Germany

(Received 3 October 1988)

The photoion-yield spectra $\sigma(X^{n+})$ with $n=1$–4 for seven elements of the lanthanides in the region of the 4*d* giant resonances between 100–200 eV were measured. Dramatic changes in the different X^{n+} signals for increasing Z show the growing influence of the 4*f* subshell in the competition between continuum transitions $4d^{10}\rightarrow 4d^{9}\epsilon f$ and discrete transitions $4d^{10}4f^{N}\rightarrow 4d^{9}4f^{N+1}$. For the analysis of the spectra the partial photoionization cross sections $\sigma(nl)$ for the subshells 4*d*, 5*s*, 5*p*, and 4*f* were calculated with the time-dependent local-density approximation.

PACS numbers: 32.80.Fb, 32.80.Dz

The photoabsorption spectra of the lanthanides in the region of 100–200 eV are characterized by strong, board, and asymmetric resonances.[1-4] These "giant" resonances, which for many years have attracted the interest of both experimental and theoretical physicists,[5] may mainly be described by the excitation of inner-shell 4*d* electrons to unoccupied 4*f* levels. The large overlap between the 4*d* and 4*f* wave functions, which causes a strong coupling of the core-excited and continuum states, and the distribution of the oscillator strengths over many resonances due to the multiplet splitting of the open shells, are the main reasons for the broad features. For a more detailed analysis of the spectra, however, one has to take into account that there are distinct differences between light and heavy lanthanides. Whereas for the light elements like La ($Z=57$) or Ce ($Z=58$) the resonances lie above the 4*d* ionization limits, the position of the resonances for increasing Z moves gradually to these limits, passes them, and for elements with $Z\geq 64$ the main part of the resonances lies below these limits. Therefore, a better description of the excitation process is $4d\rightarrow(\epsilon f,4f)$ with a mutual competition between continuum and discrete excitations. This competition can be explained by the position of the 4*f* wave function in the effective double-valley potential, which is caused by the attractive Coulombic field and the repulsive centrifugal term.[6] In neutral atoms the collapse of the 4*f* wave functions from the outer to the inner well takes place between Ba ($Z=56$) and La ($Z=57$)[7] though the 4*f* level is not occupied in the ground-state configuration of La. The removal of a 4*d* electron in the core-excited states should deepen the inner well, but due to a large exchange interaction the $4d^{9}4f\,^{1}P_{1}$ state is shifted to the outer well.[8] Therefore, the oscillator strength of the discrete transitions $4d^{10}\rightarrow 4d^{9}4f\,^{1}P_{1}$ is very small and is transferred to the continuum transitions $4d^{10}\rightarrow 4d^{9}\epsilon f\,^{1}P_{1}$, which, due to the centrifugal barrier, gives rise to a shape resonance similar to that of Xe or Ba.[9] For heavier elements the inner well gradually gets deeper so that the corresponding 4*f* wave functions in the core-excited states can collapse into the inner well and transitions to discrete states $4d^{10}4f^{N}\rightarrow 4d^{9}4f^{N+1}$ should dominate. Autoionization of these discrete states favors the super-Koster-Kronig transitions $4d^{9}4f^{N+1}\rightarrow 4d^{10}4f^{N-1}\epsilon d,g$ which can interfere with the direct 4*f* ionization $4f^{N}\rightarrow 4f^{N-1}\epsilon d,g$ yielding asymmetric resonances with Beutler-Fano profiles.[10] For a better understanding of these processes, one can study the decay of these resonances by photoelectron[5,11-14] or photoion spectroscopy. We have used monochromatized synchrotron radiation, atomic-beam technique, and a time-of-flight spectrometer to measure for the first time the partial cross sections $\sigma(X^{n+})$ for the production of lanthanide photoions X^{n+} with $n=1$–4 as a function of the photon energy in the region of the 4*d* giant resonances.

The experiments were performed at the synchrotron radiation facility of the 800-MeV electron storage ring BESSY in Berlin. The synchrotron radiation was dispersed by a toroid-grating monochromator with a 1200-lines/mm grating. The photon flux was monitored by a sodium salicylate-coated photomultiplier. The light was focused on an atomic beam emanating from an effusion oven, which was heated by electron impact. The temperatures, which were necessary for the production of a particle density of about 10^{11} atoms/cm^{3} in the interaction zone, were in the range of 1400–2000 K. For the time-of-flight technique, short pulses (120-V amplitude, 1-μs width, 25-kHz repetition rate) were applied which extracted the photoions from the interaction zone. Setting appropriate time windows, the photoions X^{n+} of different charge states with $n=1$–4 could simultaneously be detected. This method permits an accurate determination of the ratios of the photoionization cross sections $\sigma(X^{n+})$ if the collection efficiency of the differently charged ions is the same. Test experiments with Xe in the region between 80 and 180 eV showed good agreement with the results of Holland *et al.*[15] within the error limits of 20%. We have measured the photoion yield spectra $\sigma(X^{n+})$ of La, Ce, Pr, Nd, Gd, Tb, and Dy in the region of the 4*d* giant resonances. As typical examples, the spectra of La, Nd, and Dy are give in Figs. 1–3.

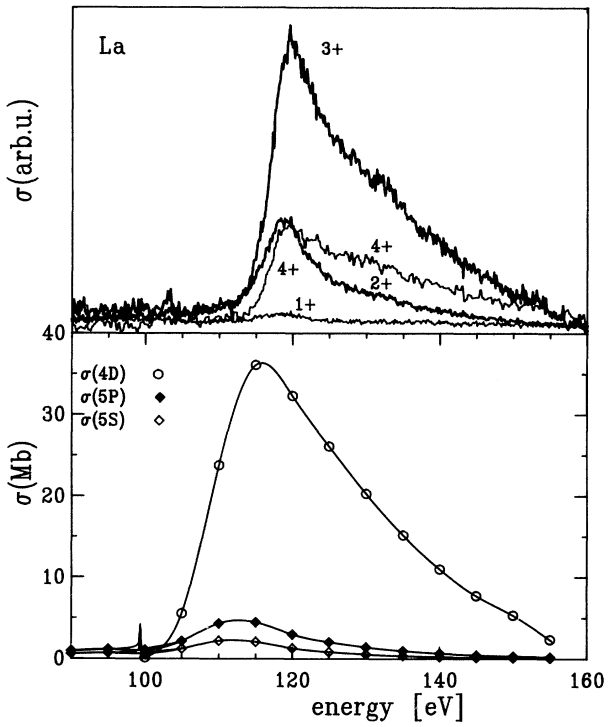

FIG. 1. Upper part: Photoion-yield spectra $\sigma(La^{n+})$ with $n=1-4$ in the region of the $4d$ giant resonances between 90 and 160 eV. Lower part: Calculated partial photoionization cross sections $\sigma(nl)$ for the subshells $4d$, $5p$, and $5s$ using TDLDA (Ref. 15).

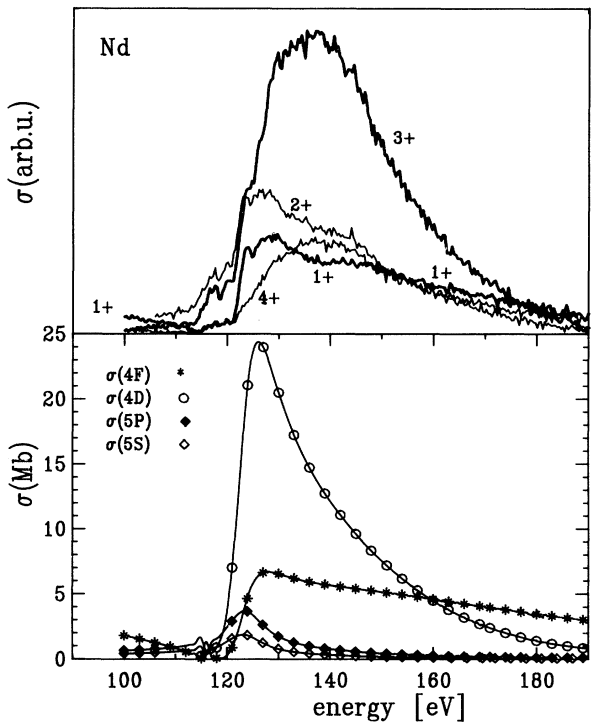

FIG. 2. Upper part: Photoion-yield spectra $\sigma(Nd^{n+})$ with $n=1-4$ in the region of the $4d$ giant resonances between 100 and 190 eV. Lower part: Calculated partial photoionization cross sections $\sigma(nl)$ for the subshells $4f$, $4d$, $5p$, and $5s$ using TDLDA (Ref. 15).

These examples were chosen to demonstrate the systematic trend for increasing Z. For the interpretation of the spectra, we have calculated the atomic partial photoionization cross sections $\sigma(nl)$ of the different subshells with a relativistic version[16] of the time-dependent local-density approximation (TDLDA).[17] Relativistic orbital energies[18] and the Gunnarsson-Lundqvist formula[19] for the exchange-correlation function were used in these calculations. The results are shown in the lower parts of Figs. 1-3.

La.—The spectra $\sigma(La^{n+})$ with $n=1-4$ are dominated by the broad shape resonance of the La^{3+} signal (Fig. 1). The weaker La^{4+} signal shows similar shape and position, whereas the La^{2+} signal is narrower and has a more symmetrical shape. Only a very small La^{+} signal is observed. If one looks at the calculated partial cross sections $\sigma(nl)$ for the subshells $4d$, $5p$, and $5s$ in the lower part of Fig. 1, these features can easily be explained: The partial cross sections $\sigma(nl)$ are dominated by the broad $\sigma(4d)$ resonance. The Auger decay of the $4d$ hole involving $5p$ or $5s$ electrons gives rise to the La^{3+} and La^{4+} signals. For example, the following decay path can lead to the production of La^{3+}:

$$La^{+}4d^{9}5s^{2}5p^{6}5d6s^{2} \rightarrow La^{2+}4d^{10}5s^{2}5p^{4}5d6s^{2} \rightarrow La^{3+}4d^{10}5s^{2}5p^{5}(5d,6s)^{1}.$$

This decay explains the corresponding Auger peak in the photoelectron spectrum.[13] Compared with $\sigma(4d)$ the partial cross sections $\sigma(5p)$ and $\sigma(5s)$ are narrower, more symmetrical, and shifted to lower energies. Therefore, the La^{2+} signal should be mainly connected with the $5p$ and $5s$ ionization. The partial cross sections $\sigma(6s)$ and $\sigma(5d)$ of the valence electrons (not shown in Fig. 1) have similar shapes and positions like $\sigma(5p)$ or $\sigma(5s)$, but are much smaller—only 5% of $\sigma(5p)$. This is the reason for the small La^{+} signal.

Nd.—As in the case of La, the triple-charge Nd ions give rise to the strongest signal in the ion-yield spectra $\sigma(Nd^{n+})$ with $n=1-4$ (Fig. 2). The corresponding Nd^{4+} signal is registered with similar shape and position. Therefore, these resonances should be explained by the partial cross section $\sigma(4d)$ although the comparison shows that the experimental curves have larger widths which may result from the actual multiplet splittings. In contrast to La, however, there is a distinct Nd^{+} signal, similar in shape and position to the Nd^{2+} signal, with a flat slope to higher photon energies, but with a minimum

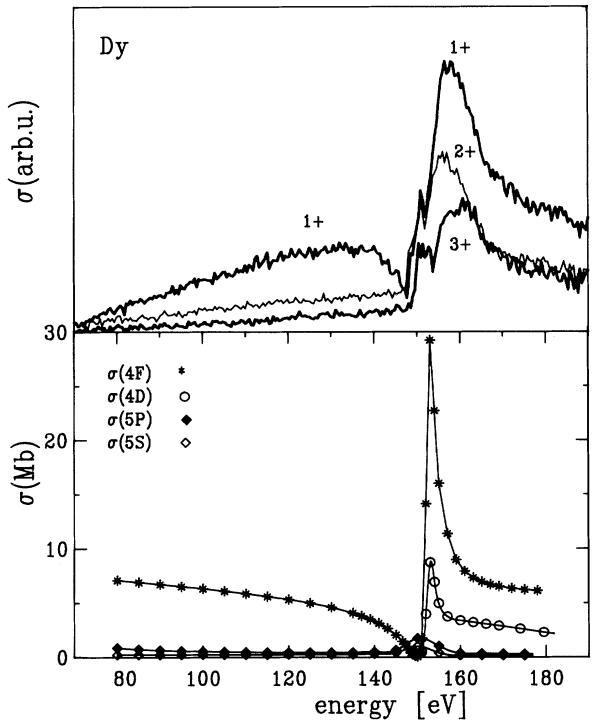

FIG. 3. Upper part: Photoion-yield spectra $\sigma(Dy^{n+})$ with $n=1-3$ in the region of the $4d$ giant resonances between 80 and 180 eV. Lower part: Calculated partial photoionization cross sections $\sigma(nl)$ for the subshells $4f$, $4d$, $5p$, and $5s$, using TDLDA (Ref. 15).

at the lower-energy part. This signal must be correlated with the electrons in the $4f$ subshell of Nd as the calculated partial cross section $\sigma(4f)$ also shows such a minimum at the low-energy part and a flat slope to higher energies.

Dy.—The increasing influence of the $4f$ subshell is very convincingly demonstrated by the spectra of Dy (Fig. 3). Here the dominating signal is the yield of single-charged Dy ions. This signal has the form of a Beutler-Fano resonance with a pronounced minimum at 144 eV. The Dy^{2+} and Dy^{3+} signals have similar resonances without such a minimum. No Dy^{4+} signal was observed within the signal-to-noise ratio of this experiment. The dominating Dy^{+} signal is very well explained by the calculated partial cross section $\sigma(4f)$. The Beutler-Fano profile indicates that the discrete transitions $4d^{10}4f^{10}\rightarrow 4d^{9}4f^{11}$ with subsequent autoionization $4d^{9}4f^{11}\rightarrow 4f^{10}4f^{9}\epsilon d,g$ dominate the spectra.

Summarizing our results, it is shown that photoion spectroscopy is a very valuable tool to study the character of the $4d$ giant resonances in the lanthanides. Whereas for the light elements the continuum transitions $4d^{10}\rightarrow 4d^{9}\epsilon f$ and the subsequent Auger decay of $4d^{-1}$ dominate the spectra with strong X^{3+} and X^{4+} signals, for the heavy elements the discrete transitions $4d^{10}4f^{N}\rightarrow 4d^{9}4f^{N+1}$ with subsequent autoionization $4d^{9}4f^{N+1}\rightarrow 4d^{10}4f^{N-1}\epsilon d,g$ are the important processes yielding strong X^{+} signals. The main features of the ion-yield spectra $\sigma(X^{n+})$ are well reproduced by the TDLDA calculations of the partial cross section $\sigma(nl)$ although there are considerable discrepancies for the exact positions, widths, and amplitudes of the resonances.

The authors thank B. Sonntag and M. Richter for many helpful conversations. This work has been funded by the German Federal Minister for Research and Technology (BMFT) under Contract No. 05 314 EX B2.

[1]M. W. D. Mansfield and J. P. Connerade, Proc. Roy. Soc. London. A **352**, 125 (1976).

[2]H.-W. Wolff, R. Bruhn, K. Radler, and B. Sonntag, Phys. Lett. **59A**, 67 (1976).

[3]E.-R. Radtke, J. Phys. B **12**, L71 (1979); **12**, L77 (1979).

[4]J. P. Connerade and M. Pantelouris, J. Phys. B **17**, L173 (1984).

[5]*Giant Resonances in Atoms, Molecules and Solids,* edited by J. P. Connerade, J. M. Esteva, and R. C. Karnatak (Plenum, New York, 1987).

[6]M. Goeppert Mayer, Phys. Rev. **60**, 184 (1941).

[7]D. C. Griffin, K. L. Andrew, and R. D. Cowan, Phys. Rev. **177**, 62 (1969).

[8]D. C. Griffin and M. S. Pindzola, Comments At. Mol. Phys. **13**, 1 (1983).

[9]F. Combet-Farnoux, in *Proceedings of the International Conference on Inner Shell Ionization Phenomena, Atlanta, Georgia, April 1972* (U.S. Atomic Energy Commission, Oak Ridge, TN, 1972), Vol. 2, p. 1130.

[10]U. Fano, Phys. Rev. **124**, 1866 (1961).

[11]M. Meyer, T. Prescher, E. v. Raven, M. Richter, E. Schmidt, B. Sonntag, and H.-E. Wetzel, Z. Phys. D **2**, 347 (1986).

[12]U. Becker, H. G. Kerkhoff, D. W. Lindle, P. H. Kobrin, T. A. Ferrett, P. A. Heimann, C. M. Truesdale, and D. A. Shirley, Phys. Rev. A **34**, 2855 (1986).

[13]D. Handschuh, M. Meyer, M. Pahler, T. Prescher, M. Richter, B. Sonntag, and H.-E. Wetzel, J. Phys. (Paris), Colloq. **48**, C9-539 (1987).

[14]M. Richter, M. Meyer, M. Pahler, T. Prescher, E. v. Raven, B. Sonntag, and H.-E. Wetzel (to be published).

[15]D. M. P. Holland, K. Codling, J. B. West, and G. V. Marr, J. Phys. B **12**, 2465 (1979).

[16]D. A. Liberman and A. Zangwill, Comput. Phys. Commun. **32**, 75 (1984).

[17]A. Zangwill and P. Soven, Phys. Rev. A **21**, 1561 (1980).

[18]K.-N. Huang, M. Aoyagi, M. H. Chen, B. Crasemann, and H. Matz, At. Data Nucl. Data Tables **18**, 243 (1976).

[19]O. Gunnarsson and B. Lundqvist, Phys. Rev. B **13**, 4274 (1976).